Weakly Nonlinear Stability Analysis of Frontal Polymerization

By L. K. Gross and V. A. Volpert

A description of frontal polymerization is given via a free boundary model with nonlinear kinetic and kinematic conditions at the free boundary. We perform a weakly nonlinear analysis for the development of pulsating instabilities on the cylinder, building on the linear stability analysis of [1]. We take as a bifurcation parameter an experimentally measurable combination of material and kinetic parameters. The asymptotic analysis leads to the derivation of an ordinary differential equation of Landau–Stuart type for the slowly varying amplitude of a linearly unstable mode. We classify nonlinear dynamics of the polymerization front by doing a parameter sensitivity study of the amplitude equation.

1. Introduction

The problem under consideration is to predict the salient features of a free-radical polymerization front. The physical problem involves a test tube

Address for correspondence: L. K. Gross, Department of Theoretical and Applied Mathematics, The University of Akron, Akron, OH 44325-4002, USA. The work of L. K. G. was supported by the National Science Foundation under Grant DMS-0074965. L. K. G. wishes to acknowledge the support of the Ohio Board of Regents (Research Challenge Grant), the Buchtel College of Arts and Sciences at The University of Akron (matching grant), and the hospitality of colleagues at Northwestern University during L. K. G.'s visit there (2001–2002). The work of V. A. V. was supported by the National Science Foundation under Grant DMS-0103856.

STUDIES IN APPLIED MATHEMATICS 110:351–375

Published by Blackwell Publishing, 350 Main Street, Malden, MA 02148, USA, and 9600 Garsington Road, Oxford, OX4 2DQ, UK.

filled with a well-mixed combination of a monomer and a thermally unstable initiator. Increasing the temperature at one end of the tube causes chemical conversion to begin. The released heat diffuses into the reactants, causing wave propagation via the usual thermal mechanism. When the initiator decomposes, radicals form and begin to combine with the monomers, forming new radicals. The new radicals then bond with other monomers, causing chains of monomers to grow. Eventually each chain combines with a second radical, terminating the growth and producing a polymeric molecule.

A comparison with self-propagating high-temperature synthesis (SHS) [2] suggests that the process described above may eventually play a role in the industrial production of polymers. In SHS, a combustion wave converts powdered ingredients into a ceramic material or metallic alloy. As with frontal polymerization (FP), the reaction is exothermic; the reaction rate depends strongly on the temperature; and the bulk of the chemical reaction and heat release occur in a narrow zone. SHS has several advantages over traditional manufacturing methods, in which the mixture is baked in a furnace. Products created by SHS are often more uniform and pure; synthesis times are shorter; and the equipment is simpler and less expensive.

In both SHS and FP, the thermal feedback between the chemical kinetics and the heat diffusion results in the sustainability of a traveling wave. In each case the uniformly propagating wave becomes unstable in certain parametric regimes.

A great variety of resulting oscillatory regimes has been documented in SHS. Shkadinsky et al. [3] predicted the simplest ones theoretically through numerical simulations on a model system of reaction-diffusion partial differential equations. The oscillations were discovered experimentally by Merzhanov et al. [4], who noted that oscillations produced layers in the burned samples normal to the front. Zeldovich et al. described this work in a monograph [5]. Many papers contain rather intricate bifurcation analyses of instabilities (see, for example, [6–9]).

Although it has been thirty years since Chechilo et al. [10] discovered frontal polymerization (in experiments in tubular chemical reactors under high pressure), stability of propagation has only recently been analyzed. Schult and Volpert did a linear stability analysis in [1].

Also, despite the fact that more than half of chemists worldwide are currently working in polymer-related areas, nonlinear dynamics of polymeric systems are still poorly understood [11]. Nevertheless, oscillatory regimes similar to those observed in SHS have begun to be detected. In 1997, Solovyov et al. [12] observed planar and nonplanar periodic modes numerically in a reaction-diffusion model of polymerization and compared the results for various kinetic schemes. They observed velocity pulsations and spin modes, which Pojman et al. [13] had seen in experiments two years earlier. Masere et al. [14] generated in subsequent experiments a period-doubling sequence that seemed to lead to chaos. As in SHS, pulsating modes were found to change the properties of the resulting product.

Our paper analyzes the behavior of the traveling wave with respect to small perturbations, taking parameter values that deviate slightly from the stability threshold. This weakly nonlinear analysis constitutes a new methodology for frontal polymerization. A parameter sensitivity study reveals nonlinear dynamics of the polymerization front. In particular, we identify some parameter ranges that produce pulsating instabilities.

The paper is organized as follows. The governing equations appear in Section 2. Section 3 contains the linear stability analysis, which also appears in [1] with one slightly different front condition and in [15], allowing for non-adiabaticity. The weakly nonlinear analysis occurs in Section 4. We focus on the situation in which the flat mode is the first mode to lose stability as the bifurcation parameter passes through the critical value.

The method follows the classical Landau–Stuart theory of hydrodynamic stability, which dates back as far as the 1940s [16–18]. The approach has been used in many different contexts. One example is a one-sided model of condensed-phase combustion on a strip with insulated edges [19, 20]. The technique was also used in [8, 21] for solid combustion on the surface of a cylinder.

The idea is to study the evolution of linearized eigenmodes modulated by complex-valued amplitude functions of independent slow time scales. Inserting a normal-mode ansatz for the temperature, monomer concentration, and interface position perturbed about a basic traveling-wave solution into the nonlinear problem and making systematic use of the method of multiple scales yields constraints on the slowly-varying amplitudes (see, for example, Kevorkian and Cole [22]).

One solvability condition implies that the amplitude A depends on the slowest time scale $t_2 = \epsilon^2 t$ only, where ϵ is a small parameter related to the deviation from the stability boundary. In the next order of the perturbation series, we obtain the Landau–Stuart equation

$$\frac{dA}{dt_2} = \mu\chi A + \beta A^2 \bar{A} \tag{1}$$

from the solvability condition. The ordinary differential equation (1) dictates the dynamics of the single unstable mode subject to self-interaction. We describe the complicated way in which χ and β in (1) depend on the kinetic and material parameters, influencing the behavior of the front.

In Section 5 we investigate the qualitative weakly nonlinear behavior of the system for the various parametric regimes. We comment on consistency with experiment.

2. Governing equations

We use a free boundary model of frontal polymerization as introduced by Goldfeder et al. [23]. It resembles the model of condensed-phase combustion which Matkowsky and Sivashinsky [24] derived as an asymptotic limit of the reaction-diffusion model for large activation energy. Although frontal polymerization is a slower and less exothermic process, the nondimensional quantities that determine the dynamics are of the same order [23], and the same asymptotic techniques apply.

In [23], equations for conservation of energy, conservation of mass, and laws of mass action describe the standard sequence of chemical reactions [25] in frontal polymerization. Simplifications follow from making a steady-state assumption, namely, the rate of change of total radical concentration is much smaller than the rates of radical production and consumption [26]. We also assume that the concentration of initiator radicals is much smaller than the concentration of growing chains of monomers and replace the distributed kinetics with two-step kinetics concentrated on the front, as in [1].

In a tube of circumference L, the reaction propagates longitudinally. Consider a fixed coordinate frame in which the direction of motion of the front is labeled $-\tilde{x}$. Because the characteristic scale of the polymerization wave is generally much smaller than the length of the tube, we consider the tube to be infinite ($-\infty < \tilde{x} < \infty$). We introduce a moving coordinate system $x = \tilde{x} - \phi(y, t)$; the front is at $x = 0$.

The dependent variables are temperature $T(x, y, t)$, monomer concentration $M(x, y, t)$, initiator concentration $I(x, y, t)$, and propagation velocity $u(y, t) = -\partial\phi(y, t)/\partial t$. The partial differential equations from [1] are

$$\frac{\partial T}{\partial t} + u\frac{\partial T}{\partial x} = \kappa\nabla^2 T, \quad \frac{\partial M}{\partial t} + u\frac{\partial M}{\partial x} = 0, \quad \frac{\partial J}{\partial t} + u\frac{\partial J}{\partial x} = 0 \tag{2}$$

on $\{(x, y, t)|x \in (-\infty, 0) \cup (0, \infty), y \in (0, L), t \in (0, \infty)\}$, where $J(x, y, t) = \sqrt{I(x, y, t)}$, κ is the thermal diffusivity, assumed to be constant, and ∇^2 is the Laplacian in the front-attached coordinate system, that is,

$$\nabla^2 = \frac{\partial^2}{\partial y^2} + \left(1 + \phi_y^2\right)\frac{\partial^2}{\partial x^2} - 2\phi_y\frac{\partial^2}{\partial x \partial y} - \phi_{yy}\frac{\partial}{\partial x}.$$

At the edges $y = 0, L$ of the domain we have periodic boundary conditions

$$T(x, 0, t) = T(x, L, t), \quad \left.\frac{\partial T}{\partial y}\right|_{y=0} = \left.\frac{\partial T}{\partial y}\right|_{y=L}, \tag{3}$$

$$\phi(0, t) = \phi(L, t), \quad \text{and} \quad \left.\frac{\partial \phi}{\partial y}\right|_{y=0} = \left.\frac{\partial \phi}{\partial y}\right|_{y=L}. \tag{4}$$

Conditions far ahead of the front are

$$\lim_{x\to-\infty} T = T_0, \quad \lim_{x\to-\infty} M = M_0, \quad \lim_{x\to-\infty} J = J_0 \tag{5}$$

and far behind the wave are

$$\lim_{x\to\infty} \frac{\partial T}{\partial x} = 0, \quad \lim_{x\to\infty} J = 0. \tag{6}$$

Front conditions derived from the sharp-interface analysis [1, 15] including curvature are

$$[T] = 0, \quad t > 0, \tag{7}$$

$$\kappa\left[\frac{\partial T}{\partial x}\right]\left(1+\left(\frac{\partial \phi}{\partial y}\right)^2\right) = q(M_0 - M_b)\frac{\partial \phi}{\partial t}, \quad t > 0, \tag{8}$$

$$\frac{\left(\frac{\partial \phi}{\partial t}\right)^2}{1+\left(\frac{\partial \phi}{\partial y}\right)^2} = F(T_b) \equiv \frac{\kappa k_{01} R_g T_b^2}{q M_0 E_1} \exp\left(\frac{J_0 A_2}{A_1} - \frac{E_1}{R_g T_b}\right)\left(\int_0^{\frac{J_0 A_2}{A_1}} \frac{e^\eta - 1}{\eta}\, d\eta\right)^{-1}, \tag{9}$$

$$M_b = f(T_b) \equiv M_0 \exp\left(-\frac{J_0 A_2}{A_1}\right). \tag{10}$$

We also have $\lim_{x\to 0^+} J = 0$. The notation above for jump in function value across $x = 0$ is defined as $[a(x)] = a(0^+) - a(0^-)$. The parameter q above is heat release, k_{01} and E_1 are the frequency factor and activation energy, respectively, related to the decomposition of the initiator, and k_{02} and E_2 are the frequency factor and activation energy, respectively, related to the polymerization. The universal gas constant is R_g. $T_b \equiv \lim_{x\to 0^+} T$ is the reaction temperature, and $M_b \equiv \lim_{x\to 0^+} M$. $A_i \equiv k_{0i} e^{-E_i/(R_g T_b)}$ is the value of the Arrhenius function for decomposition ($i = 1$) and for polymerization ($i = 2$) at the reaction zone.

In the following, we will characterize stable and unstable regimes. We will also show the role that the material and kinetic parameters play in determining the dynamics in the weakly nonlinear setting.

3. Linear stability analysis

The free boundary problem (2)–(10) admits a traveling-wave solution of speed $\hat{u}$, namely,

$$\hat{T}(x) = \begin{cases} T_0 + (\hat{T}_b - T_0)\exp\left(\frac{\hat{u}}{\kappa} x\right), & x < 0 \\ \hat{T}_b, & x > 0 \end{cases}, \tag{11}$$

$$\hat{M}(x) = \begin{cases} M_0, & x < 0 \\ \hat{M}_b, & x > 0 \end{cases}, \qquad \hat{J}(x) = \begin{cases} J_0, & x < 0 \\ 0, & x > 0 \end{cases},$$

$$\hat{\phi}(t) = -\hat{u}t.$$

The pair $(\hat{T}_b, \hat{M}_b)$ satisfies simultaneously

$$\hat{T}_b = T_0 + q(M_0 - \hat{M}_b) \quad \text{and} \quad \hat{M}_b = f(\hat{T}_b), \tag{12}$$

which follow from (8) and (10), respectively. Then,

$$\hat{u} = \sqrt{F(\hat{T}_b)}, \tag{13}$$

which follows from (9), can be calculated.

The linearization about the steady solution via $X = \hat{X} + \delta\tilde{X}, X = T, M, J, \phi$ yields

$$\mathcal{L}\tilde{T} - \frac{d\hat{T}}{dx}\left(\frac{\partial\tilde{\phi}}{\partial t} - \kappa\frac{\partial^2\tilde{\phi}}{\partial y^2}\right) = 0, \quad \frac{\partial\tilde{M}}{\partial t} + \hat{u}\frac{\partial\tilde{M}}{\partial x} = 0, \quad \frac{\partial\tilde{J}}{\partial t} + \hat{u}\frac{\partial\tilde{J}}{\partial x} = 0, \tag{14}$$

where

$$\mathcal{L}T = \frac{\partial T}{\partial t} + \hat{u}\frac{\partial T}{\partial x} - \kappa\left(\frac{\partial^2 T}{\partial x^2} + \frac{\partial^2 T}{\partial y^2}\right). \tag{15}$$

Linearized boundary conditions at the front are

$$\lim_{x\to 0^\pm} \tilde{T} + qc\frac{\partial\tilde{\phi}}{\partial t} = 0, \tag{16}$$

$$\lim_{x\to 0^+} \tilde{M} + \mathcal{P}c\frac{\partial\tilde{\phi}}{\partial t} = 0, \tag{17}$$

$$\left[\frac{\partial\tilde{T}}{\partial x}\right] - \frac{q\hat{u}c}{\kappa}(\mathcal{Z} - \mathcal{P})\frac{\partial\tilde{\phi}}{\partial t} = 0. \tag{18}$$

Also $\lim_{x\to 0^+} \tilde{J} = 0$. In the above,

$$c = \frac{M_0 - \hat{M}_b}{\hat{u}\mathcal{Z}}, \tag{19}$$

where $\mathcal{Z}$ is proportional to the logarithmic derivative of the velocity of the traveling wave with respect to the reaction temperature $\hat{T}_b$. $\mathcal{P}$ is proportional to the rate of change of the monomer concentration at the reaction front with respect to the reaction temperature $\hat{T}_b$. Specifically,

$$\mathcal{Z} = (\hat{T}_b - T_0)\frac{\partial}{\partial\hat{T}_b} \ln\hat{u}; \tag{20}$$

$$\mathcal{P} = q\frac{\partial \hat{M}_b}{\partial \hat{T}_b}. \tag{21}$$

Both $\mathcal{Z}$ and $\mathcal{P}$ can be measured experimentally. They are introduced into the problem via the substitutions

$$F'(\hat{T}_b) = \frac{2\hat{u}^2\mathcal{Z}}{\hat{T}_b - T_0}, \quad f'(\hat{T}_b) = \frac{\mathcal{P}}{q}. \tag{22}$$

The first substitution follows from the definition (20) of $\mathcal{Z}$ and the definition (13) of $\hat{u}$. The second substitution follows from the definition (21) of $\mathcal{P}$ and the expansion of $M_b = f(T_b)$ given in (10) into a Taylor series about $T_b = \hat{T}_b$.

For the linearized problem, boundary conditions on $\tilde{T}$ and $\tilde{\phi}$ at the edges $y = 0, L$ are periodic. In the far field, linearized boundary conditions are

$$\lim_{x\to-\infty} \tilde{X} = 0, \quad X = T, M, J, \quad \lim_{x\to\infty} \frac{\partial \tilde{T}}{\partial x} = 0. \tag{23}$$

Note that the front condition (16) comes from expanding condition (9) and using continuity of T (7) at the interface to get the limit as $x \to 0^-$ in addition to $x \to 0^+$. The condition (17) comes from expanding $M_b = f(T_b)$ defined in (10) and using (16) to substitute for $\tilde{T}_b = \lim_{x\to0^+} \tilde{T}$. Condition (18) comes from expanding the jump condition on $\partial T/\partial x$ in (8) and using (17) to substitute for $\tilde{M}_b = \lim_{x\to0^+} \tilde{M}$.

The normal-mode solutions

$$\tilde{T} = e^{\omega t \pm i k_j y} X_T(x;\omega,\mathcal{Z}), \quad \tilde{M} = e^{\omega t \pm i k_j y} X_M(x;\omega,\mathcal{Z}), \quad \tilde{\phi} = e^{\omega t \pm i k_j y}, \tag{24}$$

are separated-variables solutions of the linearized problem above, where $k_j = 2j\pi/L$ for the tube circumference L; $j = 0, 1, 2, \ldots$. The solutions are clockwise- and counterclockwise-traveling waves on the surface of the cylinder.

The function $X_M(x;\omega,\mathcal{Z})$ satisfies a first-order ordinary differential equation. It is piecewise continuous with the boundary condition in (23) on $\tilde{M}$ at $-\infty$ determining the constant of integration on $x < 0$ and the front condition (17) determining the constant of integration on $x > 0$. We get

$$X_M(x;\omega,\mathcal{Z}) = \begin{cases} 0, & x < 0 \\ -\omega\mathcal{P}c\exp\left(-\frac{\omega}{\hat{u}}x\right), & x > 0 \end{cases}. \tag{25}$$

Also, ω and $X_T(x;\omega,\mathcal{Z})$ satisfy a second-order eigenvalue problem. The eigenfunction is piecewise continuous with the boundary conditions in (23) on T at $\pm\infty$ determining one constant of integration on each of $x < 0$ and $x > 0$, respectively. Front conditions (16) on $\tilde{T}$ determine the remaining two constants of integration. Applying front condition (18) on $[\tilde{T}_x]$ yields the dispersion relation

$$4\Omega^3 + \left(1 + 4s_j^2 + 4\mathcal{Z} - \mathcal{Z}^2 + 2\mathcal{Z}\mathcal{P} - \mathcal{P}^2\right)\Omega^2 + \mathcal{Z}\left(1 + 4s_j^2 + \mathcal{P}\right)\Omega + s_j^2\mathcal{Z}^2 = 0, \tag{26}$$

where

$$\Omega = \frac{\kappa}{\hat{u}^2}\omega, \quad s_j = \frac{\kappa}{\hat{u}}k_j.$$

To emphasize the dependence of ω on k_j, we now write it as ω_j (and Ω as Ω_j).

The basic solution (11) loses linear stability when two complex-conjugate eigenvalues ω cross the imaginary axis at a critical value $\mathcal{Z}_c$ of $\mathcal{Z}$. By setting $\mathrm{Re}(\Omega) = 0$ in the dispersion relation (26) and eliminating $\mathrm{Im}(\Omega)$, we determine $\mathcal{Z}_c$ as a function of s_j and $\mathcal{P}$:

$$\mathcal{Z}_c = \frac{1}{C}\left\{-2s_j^2 + C(2+\mathcal{P}) \pm \sqrt{\left(2s_j^2 - C(2+\mathcal{P})\right)^2 + C^2\left(-\mathcal{P}^2 + 1 + 4s_j^2\right)}\right\},$$
$$C = 1 + 4s_j^2 + \mathcal{P}. \tag{27}$$

At $\mathcal{Z} = \mathcal{Z}_c$, two eigenvalues can be denoted as $\pm\omega_j = \pm i\psi_j$, where $\psi_j > 0$. The eigenfunction corresponding to ω_j is

$$X_T(x; i\psi_j, \mathcal{Z}_c) = -qc_c\begin{cases}\left(\frac{\hat{u}^2}{\kappa}\mathcal{Z}_c + i\psi_j\right)e^{r_+x} - \frac{\hat{u}^2}{\kappa}\mathcal{Z}_c e^{\hat{u}x/\kappa}, & x < 0\\ i\psi_j e^{r_-x}, & x > 0\end{cases}, \tag{28}$$

where

$$r_\pm = \frac{\hat{u}}{2\kappa}\left\{1 \pm \sqrt{1 + 4\left(i\frac{\kappa}{\hat{u}^2}\psi_j + s_j^2\right)}\right\}. \tag{29}$$

Here c_c is c in (19) evaluated at $\mathcal{Z} = \mathcal{Z}_c$.

Replacing s_j by a continuum of values s, we plot $\mathcal{Z}_c$ against positive s for various values of $\mathcal{P}$ to produce the neutral stability curves of Figure 1. Note that, as in many other nonlinear problems of practical interest, the curves have a minimum at a nonzero wave number. The region of stability corresponding to each neutral stability curve lies below the curve; the instability region lies above it. That is, for fixed values of s and $\mathcal{P}$, the corresponding pair of complex-conjugate eigenvalues crosses the imaginary axis in the ω plane as $\mathcal{Z}$ increases above the threshold value $\mathcal{Z}_c(s, \mathcal{P})$. Moreover, the axis is crossed transversally: $\partial\,\mathrm{Re}(\omega)/\partial\mathcal{Z} < 0$. Therefore, the loss of stability occurs through a Hopf bifurcation.

By substituting $s_j = 0$ into (27), we see that the flat mode loses stability at

$$\mathcal{Z}_c = 2 + \mathcal{P} + \sqrt{5 + 4\mathcal{P}} \equiv \mathcal{Z}^*. \tag{30}$$

Figure 1 shows that for each value of $\mathcal{P}$, there is also a second value of s at which $\mathcal{Z}_c = \mathcal{Z}^*$. In particular, by solving (27) with $\mathcal{Z}_c = \mathcal{Z}^*$, we find that, in

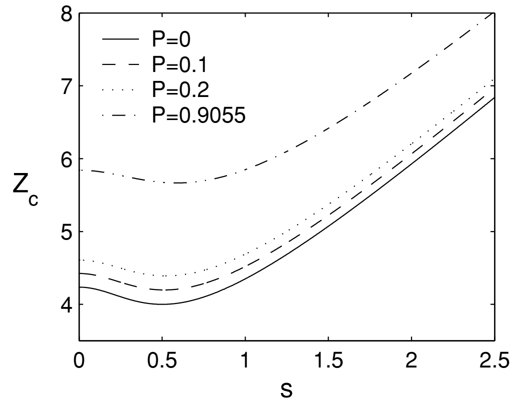

Figure 1. Neutral stability curves for $\mathcal{P}$ = 0, 0.1, 0.2, 0.9055 (bottom to top).

addition to $s_j = 0$, the mode

$$s_j = \tfrac{1}{2}\sqrt{1 + \sqrt{5 + 4\mathcal{P}}} \equiv s^* \tag{31}$$

also loses stability at $\mathcal{Z}^*$. Note from the figure that $\mathcal{Z}_c < \mathcal{Z}^*$ for $0 < s < s^*$, and $\mathcal{Z}_c > \mathcal{Z}^*$ for $s > s^*$.

Recall that we are interested in the discrete values $\pm s_j = \pm(\kappa/\hat{u})k_j = \pm 2\kappa j\pi/(\hat{u}L)$, $j = 0, 1, 2, \ldots$, which allow the normal-mode solution (24) to satisfy the periodic conditions at the edges $= 0, L$ of the strip of width L. We are thinking of a strip of width $L = 2\pi r$, where r is the radius of the tube.

If $r < \kappa/(\hat{u}s^*)$, then all modes s_j are stable for $\mathcal{Z} > \mathcal{Z}^*$. Exactly one mode ($s_0 = 0$) loses stability at $\mathcal{Z} = \mathcal{Z}^*$. Recall that $s_0 = 0$ corresponds to the dynamics with no spatial variation in the transverse direction (i.e., to the one-dimensional case). See [20] for a detailed analysis in such a case for combustion.

$\mathcal{P} = 0$ corresponds to complete conversion. Observe that in Figure 1, increasing $\mathcal{P}$ (decreasing the degree of conversion) raises the neutral stability curve. That is, increasing $\mathcal{P}$ delays the onset of instability as we increase $\mathcal{Z}$. This also eliminates some unstable modes altogether (depending on the cylinder circumference L). We see that incomplete conversion of the monomer is a stabilizing effect.

4. Weakly nonlinear analysis

In this section we consider the case in which the tube has radius $r < \kappa/(\hat{u}s^*)$, for s^* given in (31). As the parameter $\mathcal{Z}$ increases past the critical value $\mathcal{Z}^*$, the mode with wavenumber $k_0 = 0$ loses stability first.

We begin by considering a small deviation from the neutral stability curve, namely,

$$\mu\epsilon^2 = \mathcal{Z} - \mathcal{Z}^*, \tag{32}$$

for $\mathcal{Z}^*$ given in (30), and $\mu = \pm 1$. This choice of the parameter ϵ allows for the possibility of a Hopf bifurcation where the magnitude of the solution is on the order of the square root of the bifurcation parameter.

To find the neutrally stable eigenvalue $i\psi$, we evaluate the dispersion relation (26) at $s_j = 0$ and $\mathcal{Z} = \mathcal{Z}^*$ (implying $\Omega_0 = i\kappa\psi/\hat{u}^2$). Solving the real part gives

$$\psi = \frac{\hat{u}^2}{2\kappa}\sqrt{\mathcal{Z}^*(1+\mathcal{P})}. \tag{33}$$

Another quantity of interest is χ, which appears in the Landau–Stuart equation (1) governing the dynamics of the weakly unstable modes;

$$\chi \equiv \left.\frac{\partial\omega_0}{\partial\mathcal{Z}}\right|_{\mathcal{Z}=\mathcal{Z}^*} = \frac{\hat{u}^2}{\kappa}\left.\frac{\partial\Omega_0}{\partial\mathcal{Z}}\right|_{\mathcal{Z}=\mathcal{Z}^*} = \frac{\hat{u}^2\{2\kappa\psi^2(2-\mathcal{Z}^*+\mathcal{P}) - i\hat{u}^2(1+\mathcal{P})\psi\}}{-12\kappa^2\psi^2 + \hat{u}^4\mathcal{Z}^*(1+\mathcal{P})}. \tag{34}$$

The above equation follows from differentiating the dispersion relation (26) with respect to $\mathcal{Z}$ and evaluating at $s_j = 0$ and $\mathcal{Z} = \mathcal{Z}^*$ (again implying $\Omega_0 = i\kappa\psi/\hat{u}^2$).

4.1. The asymptotic strategy

The goal of this section is to find a solution to the nonlinear problem (2)–(10) of the form

$$\begin{aligned}
T(x,t,\epsilon t,\epsilon^2 t) &= \hat{T}(x) + \epsilon A(\epsilon t,\epsilon^2 t)e^{i\psi t}X_T(x;i\psi,\mathcal{Z}^*) \\
&\quad + \epsilon^2 T_2(x,t,\epsilon t,\epsilon^2 t) + \cdots + \mathrm{CC}, \\
M(x,t,\epsilon t,\epsilon^2 t) &= \hat{M} + \epsilon A(\epsilon t,\epsilon^2 t)e^{i\psi t}X_M(x;i\psi,\mathcal{Z}^*) \\
&\quad + \epsilon^2 M_2(x,t,\epsilon t,\epsilon^2 t) + \cdots + \mathrm{CC}, \\
\phi(t,\epsilon t,\epsilon^2 t) &= -\hat{u}t + \epsilon\left\{A(\epsilon t,\epsilon^2 t)e^{i\psi t} + \tfrac{1}{2}B(\epsilon t,\epsilon^2 t)\right\} \\
&\quad + \epsilon^2\phi_2(t,\epsilon t,\epsilon^2 t) + \cdots + \mathrm{CC}.
\end{aligned} \tag{35}$$

The solution involves a combination of modulations of neutrally stable solutions to the linearized problem, corresponding to $k_0 = 0$.

The asymptotic strategy is to insert first the expansions (35) into the problem (2)–(10). In addition, we expand the right-hand sides $F(T_b)$ of (9) and $f(T_b)$ of (10) in Taylor series about $T_b = \hat{T}_b$. Making the substitutions (22) introduces the parameters $\mathcal{Z}$ and $\mathcal{P}$. We then use Equation (32) to make the substitution $\mathcal{Z} = \mathcal{Z}^* + \mu\epsilon^2$. Introducing the independent time scales t,

$t_1 = \epsilon t$, and $t_2 = \epsilon^2 t$, we replace $\partial/\partial t$ by $\partial/\partial t + \epsilon\partial/\partial t_1 + \epsilon^2\partial/\partial t_2$. With these substitutions, the partial differential equation in T given in (2) becomes

$$\epsilon^2\left\{\mathcal{L}T_2 - \frac{d\hat{T}}{dx}\left(\frac{\partial\phi_2}{\partial t} - \kappa\frac{\partial^2\phi_2}{\partial y^2}\right) + \frac{\partial}{\partial t_1}\left(T_1 - \frac{d\hat{T}}{dx}\phi_1\right) - NL_1(T_1, \phi_1)\right\}$$
$$+\epsilon^3\left\{\mathcal{L}T_3 - \frac{d\hat{T}}{dx}\left(\frac{\partial\phi_3}{\partial t} - \kappa\frac{\partial^2\phi_3}{\partial y^2}\right) + \frac{\partial}{\partial t_1}\left(T_2 - \frac{d\hat{T}}{dx}\phi_2\right)\right.$$
$$\left. + \frac{\partial}{\partial t_2}\left(T_1 - \frac{d\hat{T}}{dx}\phi_1\right) - NL_2(T_1, \phi_1, T_2, \phi_2)\right\} + O(\epsilon^4) = 0, \qquad (36)$$

where $\mathcal{L}$ is given in (15). Expanding $u^2 = F(T_b)(1+\phi_y^2)$ in (9) and using $[T] = 0$ of (7) yields the front condition

$$\epsilon^2\left\{\lim_{x\to 0} T_2 + qc_c\left(\frac{\partial\phi_2}{\partial t} + \frac{\partial\phi_1}{\partial t_1}\right) - \frac{qc_c}{2\hat{u}}N_1(\phi_1)\right\}$$
$$+\epsilon^3\left\{\lim_{x\to 0} T_3 + qc_c\left(\frac{\partial\phi_3}{\partial t} + \frac{\partial\phi_2}{\partial t_1} + \frac{\partial\phi_1}{\partial t_2} - \frac{\mu}{\mathcal{Z}^*}\frac{\partial\phi_1}{\partial t}\right)\right.$$
$$\left. - \frac{qc_c}{2\hat{u}}P_1(\phi_1, \phi_2)\right\} + O(\epsilon^4) = 0. \qquad (37)$$

Expanding $M_b = f(T_b)$ in (10) and using the previous condition to substitute for higher order corrections to $\hat{T}_b$, we get the front condition

$$\epsilon^2\left\{\lim_{x\to 0^+} M_2 + \mathcal{P}c_c\left(\frac{\partial\phi_2}{\partial t} + \frac{\partial\phi_1}{\partial t_1}\right) - \frac{c_c}{2\hat{u}}N_2(\phi_1)\right\}$$
$$+\epsilon^3\left\{\lim_{x\to 0^+} M_3 + \mathcal{P}c_c\left(\frac{\partial\phi_3}{\partial t} + \frac{\partial\phi_2}{\partial t_1} + \frac{\partial\phi_1}{\partial t_2} - \frac{\mu}{\mathcal{Z}^*}\frac{\partial\phi_1}{\partial t}\right)\right.$$
$$\left. - \frac{c_c}{2\hat{u}}P_2(\phi_1, \phi_2)\right\} + O(\epsilon^4) = 0. \qquad (38)$$

Expanding the jump condition (8) on T_x and using the previous condition to substitute for higher order corrections to $\hat{M}_b$, we get the front condition

$$\epsilon^2\left\{\left[\frac{\partial T_2}{\partial x}\right] - \frac{q\hat{u}c_c}{\kappa}(\mathcal{Z}^* - \mathcal{P})\left(\frac{\partial\phi_2}{\partial t} + \frac{\partial\phi_1}{\partial t_1}\right) - \frac{qc_c}{\kappa}N_3(\phi_1)\right\}$$
$$+\epsilon^3\left\{\left[\frac{\partial T_3}{\partial x}\right] - \frac{q\hat{u}c_c}{\kappa}(\mathcal{Z}^* - \mathcal{P})\left(\frac{\partial\phi_3}{\partial t} + \frac{\partial\phi_2}{\partial t_1} + \frac{\partial\phi_1}{\partial t_2}\right)\right.$$
$$\left. - \frac{q\hat{u}c_c\mu}{\kappa}\frac{\mathcal{P}}{\mathcal{Z}^*}\frac{\partial\phi_1}{\partial t} - \frac{qc_c}{\kappa}P_3(\phi_1, \phi_2)\right\} + O(\epsilon^4) = 0. \qquad (39)$$

Here T_j, M_j, and ϕ_j are the $O(\epsilon^j)$ perturbations of T, M, and ϕ, respectively, given in (35), and c_c is given by the expression (19) for c evaluated at $\mathcal{Z} = \mathcal{Z}^*$. Terms labeled NL_j are nonlinear functions of the arguments indicated (see Appendix A). Terms labeled N_j and P_j are nonlinear functions of the forms

$$\begin{aligned} N_j &= N_{j1}\left(\frac{\partial\phi_1}{\partial t}\right)^2 + N_{j2}\left(\frac{\partial\phi_1}{\partial y}\right)^2, \\ P_j &= P_{j1}\frac{\partial\phi_1}{\partial t}\left(\frac{\partial\phi_2}{\partial t} + \frac{\partial\phi_1}{\partial t_1}\right) + P_{j2}\left(\frac{\partial\phi_1}{\partial t}\right)^3 + P_{j3}\frac{\partial\phi_1}{\partial t}\left(\frac{\partial\phi_1}{\partial y}\right)^2 \\ &\quad + P_{j4}\frac{\partial\phi_1}{\partial y}\frac{\partial\phi_2}{\partial y}. \end{aligned} \tag{40}$$

(See Appendix A for the coefficients.)

Equating like powers of ϵ results in subproblems for the terms in the perturbation expansions (35). Note that no $O(1)$ terms appear in the expanded problem (36)–(39) because in (35) we took the temperature-concentration-interface triple (T, M, ϕ) perturbed about $(\hat{T}(x), \hat{M}(x), -\hat{u}t)$, a solution to the nonlinear problem (2)–(10).

Similarly, no $O(\epsilon)$ terms appear in the expanded problem (36)–(39). The $O(\epsilon)$ problem is just the linearized problem (14)–(23) with $\mathcal{Z} = \mathcal{Z}^*$. It is satisfied identically by the $O(\epsilon)$ terms in the expansions (35) of T, M, ϕ, namely,

$$\begin{aligned} T_1(x, t, \epsilon t, \epsilon^2 t) &= A(\epsilon t, \epsilon^2 t)e^{i\psi t}X_T(x; i\psi, \mathcal{Z}^*) + \text{CC}, \\ M_1(x, t, \epsilon t, \epsilon^2 t) &= A(\epsilon t, \epsilon^2 t)e^{i\psi t}X_M(x; i\psi, \mathcal{Z}^*) + \text{CC}, \\ \phi_1(t, \epsilon t, \epsilon^2 t) &= \left\{A(\epsilon t, \epsilon^2 t)e^{i\psi t} + \tfrac{1}{2}B(\epsilon t, \epsilon^2 t)\right\} + \text{CC}. \end{aligned} \tag{41}$$

We will examine the $O(\epsilon^2)$ and $O(\epsilon^3)$ subproblems in Sections 4.3 and 4.4. In order to have bounded solutions, the subproblems will have to satisfy integral solvability conditions. The conditions will lead in turn to differential equations in the amplitudes A and B.

For the $O(\epsilon^2)$ problem, one such differential equation will show that the complex amplitude A depends on the slowest time scale t_2 only. The other will result in an expression for B in terms of A. Solving the $O(\epsilon^2)$ problem subject to these differential equations will give the forms of T_2 and ϕ_2 with A still unknown. The solvability condition on the $O(\epsilon^3)$ problem will lead to the ordinary differential equation (1), which will determine the dynamics of the unstable modes.

4.2. Solvability conditions

The $O(\epsilon^j)$ subproblems included in (36)–(39), $j = 2, 3$, can be written as

$$\mathcal{L}T_j - \frac{d\hat{T}}{dx}\left(\frac{\partial \phi_j}{\partial t} - \kappa \frac{\partial^2 \phi_j}{\partial y^2}\right) = \hat{Q}_j(x, y, \mathbf{t}), \tag{42}$$

$$\lim_{x \to 0} T_j + q c_c \frac{\partial \phi_j}{\partial t} = \hat{\alpha}_j(y, \mathbf{t}), \tag{43}$$

$$\lim_{x \to 0^+} M_j + \mathcal{P} c_c \frac{\partial \phi_j}{\partial t} = \beta_j(y, \mathbf{t}), \tag{44}$$

$$\left[\frac{\partial T_j}{\partial x}\right] - \frac{q \hat{u} c_c}{\kappa}(\mathcal{Z}^* - \mathcal{P})\frac{\partial \phi_j}{\partial t} = \hat{\gamma}_j(y, \mathbf{t}), \tag{45}$$

where $\mathbf{t} = (t, t_1, t_2)$, and we have named the right-hand sides above as $\hat{Q}_j$, $\hat{\alpha}_j$, β_j, and $\hat{\gamma}_j$.

To obtain solvability conditions for the perturbed problem in Section 4, we first take the inner product of the partial differential equation (42) with a test function v, namely,

$$\left(\mathcal{L}T_j - \frac{d\hat{T}}{dx}\left(\frac{\partial \phi_j}{\partial t} - \kappa \frac{\partial^2 \phi_j}{\partial y^2}\right), v\right) = (Q_j(\xi, \eta, \mathbf{t}), v), \tag{46}$$

where we define the inner product of two functions u and v as

$$(u, v) = \lim_{t_f \to \infty} \frac{1}{t_f} \int_0^{t_f} \int_0^L \int_{-\infty}^{\infty} u(\xi, \eta, \tau)\overline{v(\xi, \eta, \tau)}\, d\xi\, d\eta\, d\tau. \tag{47}$$

Throughout this section, we assume that $T_j, v \in L^2(D)$, where $D = \{(x, y, t)|\ 0 \le y \le L, -\infty < x < \infty, 0 \le t < \infty\}$, and that T_j and v are bounded on D. The function $\phi_j(y, t) \in L^2([0, L] \times [0, \infty))$ and is bounded on that set.

We define the adjoint problem by integrating (46) by parts appropriately, applying the conditions (23) at $x = \pm\infty$, and applying the definition of $\hat{T}(x)$ in (11). For the problem retaining y dependence, we also apply the periodic conditions (3) on T_j at $y = 0, L$. The function v is in the nullspace of the adjoint operator if

$$\mathcal{L}^* v = -v_t - \kappa(v_{yy} + v_{xx}) - \hat{u} v_x = 0, \tag{48}$$

and v satisfies

$$v|_{y=0} = v|_{y=L}, \quad \left.\frac{\partial v}{\partial y}\right|_{y=0} = \left.\frac{\partial v}{\partial y}\right|_{y=L}, \tag{49}$$

$$[v] = 0, \quad \lim_{x \to -\infty} \frac{\partial v}{\partial x} = 0, \quad \text{and} \quad \lim_{x \to \infty} v = 0. \tag{50}$$

Then the inner product (46) reduces to

$$\lim_{t_f\to\infty}\frac{1}{t_f}\int_0^{t_f}\int_0^L\left(\left[\frac{\partial T_j}{\partial x}\right]\kappa\bar{v}|_{x=0}-\kappa T_j|_{x=0}\left[\frac{\partial\bar{v}}{\partial x}\right]\right.$$
$$\left.-\phi_j q(M_0-\hat{M}_b)\hat{u}\frac{\partial\bar{v}}{\partial x}\bigg|_{x=0^-}\right)d\eta\;d\tau$$
$$=\lim_{t_f\to\infty}\frac{1}{t_f}\int_0^{t_f}\int_0^L\int_{-\infty}^{\infty}\hat{Q}_j(\xi,\eta,\mathbf{t})\bar{v}\;d\xi\;d\eta\;d\tau,$$

where $\hat{u}^2=F(\hat{T}_b)$ as given in (13). When front conditions (43) and (45) are applied to the equation above and we integrate by parts in t, we get the last boundary condition for the adjoint problem:

$$(\mathcal{Z}^*-\mathcal{P})\left.\frac{\partial v}{\partial t}\right|_{x=0}+\mathcal{Z}^*\hat{u}\left.\frac{\partial v}{\partial x}\right|_{x=0^-}+\frac{\kappa}{\hat{u}}\left[\frac{\partial^2 v}{\partial x\partial t}\right]=0. \tag{51}$$

The solvability condition is

$$\lim_{t_f\to\infty}\frac{\kappa}{t_f}\int_0^{t_f}\int_0^L\left(\hat{\gamma}_j(\eta,\mathbf{t})\bar{v}|_{x=0}-\hat{\alpha}_j(\eta,\mathbf{t})\left[\frac{\partial\bar{v}}{\partial x}\right]\right)d\eta\;d\tau$$
$$=\lim_{t_f\to\infty}\frac{1}{t_f}\int_0^{t_f}\int_0^L\int_{-\infty}^{\infty}\hat{Q}_j(\xi,\eta,\mathbf{t})\bar{v}\;d\xi\;d\eta\;d\tau, \tag{52}$$

where $\hat{Q}_j$, $\hat{\alpha}_j$, and $\hat{\gamma}_j$ are right-hand sides in conditions (42)–(45). Note that the equation in (2) in M is solvable without a special condition such as (52).

Solving the partial differential equation (48) by separation of variables, subject to the periodic conditions in (49) on v, allows the y-dependent $v_\pm$:

$$v_\pm=e^{i(l_jt\pm k_jy)}h(x;il_j),\quad k_j=2j\pi/L,\quad j=0,1,2,\dots, \tag{53}$$

where $h(x;il_j)$ satisfies

$$\kappa h''+\hat{u}h'-\left(\kappa k_j^2-il_j\right)h=0. \tag{54}$$

Applying conditions (51) on v implies that we must have

$$[h]=0,\quad \lim_{x\to-\infty}\frac{dh}{dx}=0,\quad\text{and}\quad\lim_{x\to\infty}h=0. \tag{55}$$

Applying condition (51) yields $l_j=\psi_j$, where $\Omega=\kappa\psi_j/\hat{u}^2$ satisfies the dispersion relation (26).

Therefore, the adjoint eigenfunction is

$$h(x;i\psi_j)=\begin{cases}\exp\left(\frac{\hat{u}}{2\kappa}\left\{-1+\sqrt{1+4\left(-\frac{\kappa}{\hat{u}^2}i\psi_j+\frac{\kappa^2}{\hat{u}^2}k_j^2\right)}\right\}x\right), & x<0\\ \exp\left(\frac{\hat{u}}{2\kappa}\left\{-1-\sqrt{1+4\left(-\frac{\kappa}{\hat{u}^2}i\psi_j+\frac{\kappa^2}{\hat{u}^2}k_j^2\right)}\right\}x\right), & x>0\end{cases}, \quad (56)$$

where we have taken the arbitrary normalization constant to be 1. A solution to the adjoint of the linearized problem is

$$v_{\pm}(x,y,t;i\psi_j)=e^{i(\psi_j t\pm k_j y)}h(x;i\psi_j). \quad (57)$$

We will focus on the case $k_j=0$ in the subsequent sections.

Note that if $j=0$ then $k_j=0$, and $\psi_j=0$ is also an eigenvalue. Another adjoint solution is

$$v_0(x,y,t;0)=\begin{cases}1, & x<0\\ \exp\left(-\frac{\hat{u}}{\kappa}x\right), & x>0\end{cases}. \quad (58)$$

The presence of this trivial eigenvalue is due to the invariance of the original problem with respect to a shift in the x direction. Only the front velocity, not its position, enters the formulation of the direct problem.

4.3. The $O(\epsilon^2)$ problem

Solvability conditions for the $O(\epsilon^2)$ problem will show that the complex amplitude A depends on the slowest time scale t_2 only and will lead to an expression for B in terms of A. In addition, solving the $O(\epsilon^2)$ problem we will obtain the forms of T_2 and ϕ_2 with A still unknown.

Substituting y-independent T_1, M_1, and ϕ_1 as given in (41), the $O(\epsilon^2)$ subproblem included in (36)–(39) can be written as (42)–(45) for $j=2$, where the inhomogeneous terms have the forms

$$\hat{Q}_2(x,\mathbf{t})=\left(-\frac{\partial A}{\partial t_1}e^{i\psi t}\left(X_T(x;i\psi,\mathcal{Z}^*)-\frac{d\hat{T}}{dx}\right)\right.$$
$$\left.+A^2e^{2i\psi t}i\psi\frac{dX_T}{dx}-A\bar{A}i\psi\frac{dX_T}{dx}+\mathrm{CC}\right)+\frac{\partial B}{\partial t_1}\frac{d\hat{T}}{dx}, \quad (59)$$

$$\hat{\alpha}_2(\mathbf{t})=-qc_c\left\{\left(\frac{\partial A}{\partial t_1}e^{i\psi t}+A^2e^{2i\psi t}\left(\frac{N_{11}}{2\hat{u}}\psi^2\right)\right.\right.$$
$$\left.\left.-A\bar{A}\left(\frac{N_{11}}{2\hat{u}}\psi^2\right)+\mathrm{CC}\right)+\frac{\partial B}{\partial t_1}\right\}, \quad (60)$$

$$\hat{\gamma}_2(\mathbf{t}) = \frac{qc_c}{\kappa}\left\{\left(\hat{u}(\mathcal{Z}^* - \mathcal{P})\frac{\partial A}{\partial t_1}e^{i\psi t} + A^2 e^{2i\psi t}\left(-N_{31}\psi^2\right)\right.\right.$$
$$\left.\left. + A\bar{A}\left(N_{31}\psi^2\right) + \mathrm{CC}\right) + \hat{u}(\mathcal{Z}^* - \mathcal{P})\frac{\partial B}{\partial t_1}\right\}, \tag{61}$$

where ψ is given in (33). Expanding boundary conditions (5)–(6) and equating $O(\epsilon^2)$ terms, we get

$$\lim_{x\to-\infty} T_2 = 0, \quad \lim_{x\to\infty}\frac{\partial T_2}{\partial x} = 0. \tag{62}$$

The problem must satisfy the solvability condition (52) for $j = 2$ and $v = v_\pm$ as defined in (57) with $k_j = 0$. Integrating by parts in x, the solvability condition can be expressed as a nonzero coefficient times dA/dt_1 equals zero, implying

$$\frac{\partial A}{\partial t_1} = 0. \tag{63}$$

That is, the amplitude A depends on the slowest time scale t_2 only.

Similarly, the solvability condition (52) for $j = 2$ must be satisfied for $v = v_0$ as defined in (58). Using the reasoning outlined above, the solvability condition (52) can be expressed as

$$\frac{\partial B}{\partial t_1} = -2A\bar{A}r_0, \quad r_0 = -\frac{\psi^2}{\hat{u}(1+\mathcal{P})}\left(\frac{\hat{u}}{\kappa}\,\mathrm{Re}\left(\frac{1}{r_+}\right) + \frac{N_{11}}{2} + N_{31}\right), \tag{64}$$

where r_+ is the expression in (29) evaluated at $s_j = 0$ and $\psi_j = \psi$, and the N_{ij} are given in Appendix A.

Applying the conditions (63) and (64) puts the $O(\epsilon^2)$ problem in a solvable form. In particular, we get (42)–(45) for $j = 2$ with the right-hand sides that do not produce secular terms, namely,

$$\mathcal{L}T_2 - \frac{d\hat{T}}{dx}\left(\frac{\partial\phi_2}{\partial t} - \kappa\frac{\partial^2\phi_2}{\partial y^2}\right) = A^2 e^{2i\psi t}R_2(x) + A\bar{A}R_0(x) + \mathrm{CC},$$

$$\lim_{x\to 0} T_2 + qc_c\frac{\partial\phi_2}{\partial t} = A^2 e^{2i\psi t}F_2 + A\bar{A}F_0 + \mathrm{CC},$$

$$\left[\frac{\partial T_2}{\partial x}\right] - \frac{q\hat{u}c_c}{\kappa}(\mathcal{Z}^* - \mathcal{P})\frac{\partial\phi_2}{\partial t} = A^2 e^{2i\psi t}G_2 + A\bar{A}G_0 + \mathrm{CC},$$

and (44) in M_2, where

$$R_j(x) = -(-1)^{j/2}i\psi X_T'(x; i\psi, \mathcal{Z}^*) - r_j\hat{T}'(x),$$
$$F_j = qc_c\left\{(-1)^{j/2}\frac{N_{11}}{2\hat{u}}\psi^2 + r_j\right\},$$
$$G_j = \frac{qc_c}{\kappa}\left\{(-1)^{j/2}N_{31}\psi^2 - \hat{u}(\mathcal{Z}^* - \mathcal{P})r_j\right\},$$

$j = 0, 2$, for r_0 given in (64), and $r_2 = 0$. Note that boundary condition (44) required no modifications to the right-hand side $\beta(y, \mathbf{t})$; it does not lead to secular terms.

Temperature and interface solutions have the forms

$$T_2(x, \mathbf{t}) = A^2 e^{2i\psi t} g_2(x) + A\bar{A} g_0(x) + \text{CC}, \tag{65}$$

$$\phi_2(\mathbf{t}) = A^2 e^{2i\psi t} C_2 + \text{CC}. \tag{66}$$

The functions $g_2(x)$, $g_0(x)$, and the constant C_2 are defined in Appendix B. They satisfy the initial-value problems

$$\kappa g_j'' - \hat{u} g_j' - ij\psi g_j = -ij\psi \hat{T}'(x) C_2 - R_j(x), \tag{67}$$

$$g_j(0) = -ij\psi q c_c C_2 + F_j, \tag{68}$$

$$[g_j'(x)] = ij\psi \frac{q c_c \hat{u}}{\kappa} (\mathcal{Z}^* - \mathcal{P}) C_2 + G_j, \tag{69}$$

$$\lim_{x \to \infty} g_j'(x) = 0,$$

$$\lim_{x \to -\infty} \text{Re}(g_0(x)) = 0,$$

$$\lim_{x \to -\infty} g_2(x) = 0.$$

4.4. The $O(\epsilon^3)$ problem

Solvability conditions for the $O(\epsilon^3)$ problem will lead to an ordinary differential equation for the slowly varying amplitude A. When we substitute T_1, M_1, ϕ_1, T_2, M_2, and ϕ_2 into the expanded problem (36)–(39), the $O(\epsilon^3)$ subproblem can be written as (42)–(45) for $j = 3$, where the inhomogeneous terms have the forms

$$\hat{Q}_3(x, \mathbf{t}) = e^{i\psi t} \left\{ \frac{dA}{dt_2} \left(-X_T(x; i\psi, \mathcal{Z}^*) + \hat{T}'(x) \right) + A^2 \bar{A} R_1(x) \right\} + \mathcal{T}, \tag{70}$$

$$\hat{\alpha}_3(\mathbf{t}) = e^{i\psi t} \left\{ q c_c \left(-\frac{dA}{dt_2} + \frac{\mu}{\mathcal{Z}^*} i\psi A \right) + A^2 \bar{A} F_1 \right\} + \mathcal{T}, \tag{71}$$

$$\hat{\gamma}_3(\mathbf{t}) = e^{i\psi t} \left\{ \frac{q c_c}{\kappa} \left(\hat{u} (\mathcal{Z}^* - \mathcal{P}) \frac{dA}{dt_2} + \mu \hat{u} \frac{\mathcal{P}}{\mathcal{Z}^*} i\psi A \right) + A^2 \bar{A} G_1 \right\} + \mathcal{T}. \tag{72}$$

Here $\mathcal{T}$ stands for non-secular terms, and

$$R_1(x) = 2C_2 i\psi \bar{X}_T'(x; i\psi, \mathcal{Z}^*) - 2r_0 X_T'(x; i\psi, \mathcal{Z}^*) + 2i\psi\ \text{Re}(g_0'(x)) - i\psi g_2'(x),$$

$$F_1 = \frac{q c_c \psi}{2\hat{u}} \left\{ P_{11}(-2r_0 i + 2\psi C_2) + 3P_{12} i\psi^2 \right\},$$

$$G_1 = \frac{q c_c \psi}{\kappa} \left\{ P_{31}(-2r_0 i + 2\psi C_2) + 3P_{32} i\psi^2 \right\}.$$

Expanding boundary conditions (5)–(6), and equating $O(\epsilon^3)$ terms, we get

$$\lim_{x\to-\infty} T_2 = 0, \quad \lim_{x\to\infty} \frac{\partial T_2}{\partial x} = 0.$$

The problem must satisfy the solvability condition (52) for $v = v_\pm$ as defined in (57) and (56). Simplifying the integrals as in the previous section yields the Landau–Stuart equation

$$\frac{dA}{dt_2} = \mu\chi A + \beta A^2 \bar{A}, \tag{73}$$

where χ is given in (34), and

$$\beta = -\frac{\kappa(G_1\bar{h}(0) - F_1[\bar{h}'(x)]) - \int_{-\infty}^{\infty} R_1(\xi)\bar{h}(\xi)\,d\xi}{qc_c(\hat{u}(\mathcal{Z}^* - \mathcal{P})\bar{h}(0) + \kappa[\bar{h}'(x)]) + \int_{-\infty}^{\infty}\big(X_T(\xi; i\psi, \mathcal{Z}^*) - \hat{T}'(\xi)\big)\bar{h}(\xi)\,d\xi}.$$

Here $h(x) \equiv h(x; i\psi)$ is the adjoint eigenfunction (56), for ψ given in (33). Recall $X_T(x; i\psi_j, \mathcal{Z}_c)$ is given in (28).

Note that β depends on the kinetics in a complicated way, as F_1 and G_1 depend on derivatives of $F(T_b)$ and $f(T_b)$ in (9) and (10) evaluated at $T_b = \hat{T}_b$, and $R_1(x)$ depends on solutions (B.1) to the initial-value problems of Section 4.3.

5. Asymptotic dynamics

In this section we use the Landau–Stuart equation (73) to make predictions about the dynamical evolution of the polymerization front for a $\mathcal{Z}$ value $O(\epsilon^2)$ above or below the critical value as in (32). The amplitude equation (73) completely determines the dynamics of the weakly unstable mode

$$A(t_2)e^{i\psi t}, \tag{74}$$

subject to nonlinear self-interaction.

To investigate the dynamics, we first rewrite the Landau–Stuart equation (73) in terms of the magnitude of the complex amplitude via the substitution $A(t_2) = |A(t_2)|e^{i\theta(t_2)}$. Equating the real parts yields

$$\frac{d|A|}{dt_2} = |A|(\mu\,\mathrm{Re}(\chi) + |A|^2\,\mathrm{Re}(\beta)). \tag{75}$$

Perturbation amplitude $|A| = 0$ is a stationary solution for (75). One can easily prove using equations (34), (33), and (30) that $\mathrm{Re}(\chi) > 0$ for all physical values of the parameters. Consequently, for the ordinary differential equation (75), trajectories with an initial point close to $|A| = 0$ tend toward $|A| = 0$ in the stable setting $\mu = -1$, where μ is defined in (32). The basic solution is recovered in the limit.

By contrast, if $\mu = 1$, trajectories with an initial point near the origin in the complex A plane tend away from the origin. That is, in the absence of other equilibria, the amplitude blows up in (slow) time for $\mathcal{Z}$ slightly above the critical value.

However, equation (75) does have a second equilibrium $|A| = \sqrt{-\mu\,\mathrm{Re}(\chi)/\mathrm{Re}(\beta)}$ if $\mu/\mathrm{Re}(\beta)$ is negative. In the weakly nonlinear regime, $\mathrm{Re}(\beta)$ is negative for all physically relevant parameter values that we considered, as discussed below. Therefore, circular limit cycles $|A| = \sqrt{-\mu\,\mathrm{Re}(\chi)/\mathrm{Re}(\beta)}$ exist in the unstable case $\mu = 1$. A supercritical Hopf bifurcation occurs at $\mathcal{Z} = \mathcal{Z}^*$.

A simple stability analysis of (75) shows that $d|A|/dt_2 < 0$ outside of the circle $|A| = \sqrt{-\mu\,\mathrm{Re}(\chi)/\mathrm{Re}(\beta)}$, and $d|A|/dt_2 > 0$ inside it. The limit cycles are asymptotically stable. The nonlinear solution develops oscillations of magnitude $O(\epsilon)$ on the time scale $O(\epsilon^{-2})$.

To illustrate that $\mathrm{Re}(\beta) < 0$ in a wide class of parameter regimes, Figure 2 shows a graph of b versus $j_0 = J_0 k_{02}/k_{01}$, where nondimensional

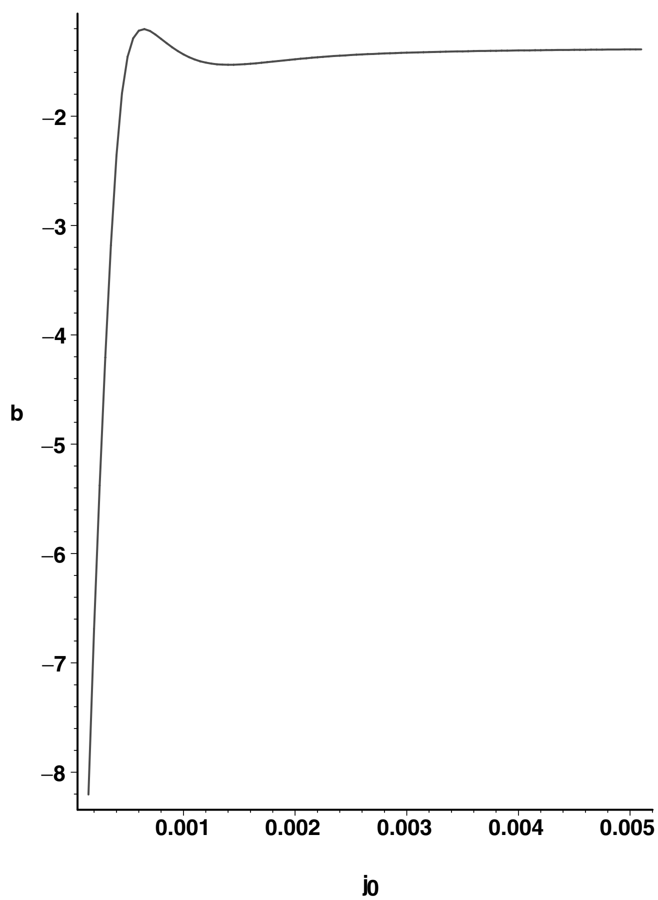

Figure 2. Graph of dimensionless $b = \mathrm{Re}(\beta)\kappa^3/\hat{u}^4$ versus dimensionless $j_0 = J_0 k_{02}/k_{01}$.

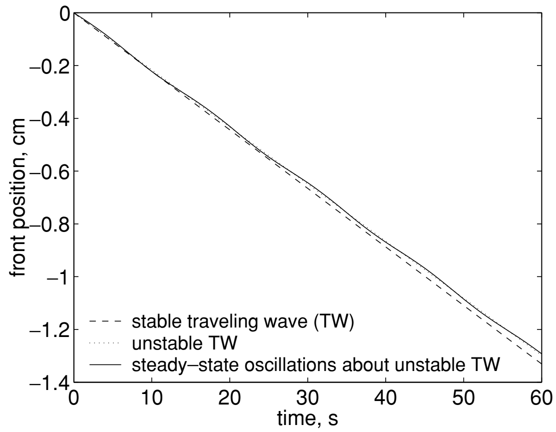

Figure 3. Front position in (35) as a function of time up to $O(\epsilon)$, where $\epsilon = 0.1$; $t = 0$ corresponds to onset of steady-state behavior.

$b = \mathrm{Re}(\beta)\kappa^3/\hat{u}^4$. Also,

$$\frac{E_1 - E_2}{R_g q M_0} = 19.79; \quad \frac{E_1}{R_g q M_0} = 58.4. \tag{76}$$

The diffusivity constant κ remains free, and initial temperature T_0 is chosen so that $\mathcal{Z}$ is the neutrally stable value $\mathcal{Z}^*$. We note that $\mathrm{Re}(\beta)$ does not change sign if T_0 is increased (decreased) such that $\mathcal{Z}$ is decreased (increased) to a value $O(\epsilon^2)$ below (above) $\mathcal{Z}^*$.

Figures 3 and 4 illustrate the oscillatory solutions that develop in the weakly unstable regimes. In Figures 3 and 4, parameter values are as in [1], namely,

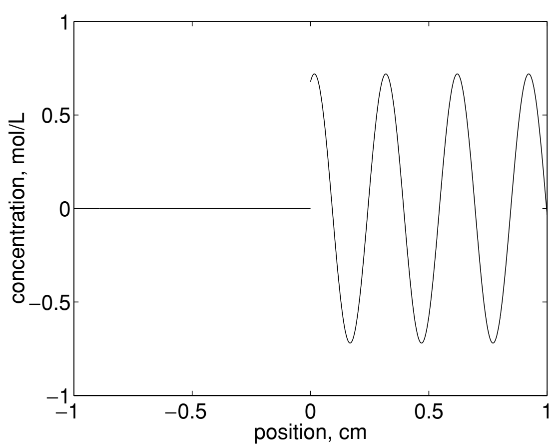

Figure 4. Leading-order correction in (41) to the basic state monomer concentration as a function of the spatial variable at a given time in the pulsating regime.

$$
\begin{aligned}
q &= 33.24 \text{ L K/mol}, & M_0 &= 7 \text{ mol/L}, \\
I_0 &= 0.1 \text{ mol/L}, & \kappa &= 0.0014 \text{ cm}^2\text{/s}, \\
E_1 &= 27 \text{ kcal/mol}, & E_2 &= 17.85 \text{ kcal/mol}, \\
k_{01} &= 2 \times 10^{12} \text{ 1/s}, & k_{02} &= 1.83 \times 10^9 \sqrt{\text{L/mol}}\text{/s}.
\end{aligned}
\tag{77}
$$

(They are consistent with the values (76) of Figure 2.)

The solid line in Figure 3 shows the pulsating front position for T_0 chosen such that $\mathcal{Z} = \mathcal{Z}^* + \epsilon^2$. The function is $-\hat{u}t + \epsilon[A(\epsilon t, \epsilon^2 t)e^{i\psi t} + \text{CC} + B(\epsilon t, \epsilon^2 t)]$, as given in (35), where the differential equation (64) defines B. The dashed line is the stable traveling wave $-\hat{u}t$ for T_0 chosen such that $\mathcal{Z} = \mathcal{Z}^* - \epsilon^2$. Figure 4 shows an $O(\epsilon)$ perturbation M_1 of monomer concentration given in (41). It has an oscillatory character behind the reaction front.

6. Conclusions

In this paper we have performed a weakly nonlinear analysis of sharp polymerization fronts that propagate in a test tube, focusing on the case of a flat interface. The asymptotic analysis led to the derivation of a Landau–Stuart equation for the slowly varying amplitude of the weakly linearly unstable mode. The ordinary differential equation resulted from the application of a solvability condition to the $O(\epsilon^3)$ problem.

By analyzing the dynamics of the Landau–Stuart equation, we identified periodic pulsations of the front for a range of parameter values. Figure 2 shows that as the initial concentration of the initiator increases (or the decomposition frequency of the initiator decreases), the dimensionless $\text{Re}(\beta)$ approaches an $O(1)$ limiting value. (In fact, convergence is very rapid.) Consequently, the amplitude $\sqrt{-\text{Re}(\chi)/\text{Re}(\beta)}$ approaches a constant.

This limiting regime as $j_0 = J_0 k_{02}/k_{01}$ tends to infinity corresponds to a well-known model of condensed-phase combustion. Our detection of a supercritical bifurcation is consistent with a similar analysis [24] in condensed-phase combustion. As mentioned in Section 1, the accompanying oscillations have been detected experimentally in self-propagating high temperature synthesis.

Figure 2 shows that for small values of j_0, on the other hand, $\text{Re}(\beta)$ increases sharply in absolute value. As a result, the amplitude $\sqrt{-\text{Re}(\chi)/\text{Re}(\beta)}$ approaches zero.

One might expect these small one-dimensional pulsations to be hard to detect experimentally, and, indeed, they have not been observed in frontal polymerization. Figure 3 emphasizes that it is difficult to distinguish such oscillations from a stable traveling wave.

Appendix A. Nonlinear functions in the expanded problem

The coefficients in the nonlinear functions (41) in the expanded problem (36)–(39) are

$$NL_1(T_1,\phi_1) = \frac{\partial T_1}{\partial x}\left(\frac{\partial \phi_1}{\partial t} - \kappa\frac{\partial^2\phi_1}{\partial y^2}\right) - 2\kappa\frac{\partial\phi_1}{\partial y}\frac{\partial^2 T_1}{\partial y\partial x} + \kappa\frac{d^2\hat{T}}{dx^2}\left(\frac{\partial\phi_1}{\partial y}\right)^2,$$

$$\begin{aligned}NL_2(T_1,\phi_1,T_2,\phi_2) = {}& 2\kappa\frac{d^2\hat{T}}{dx^2}\frac{\partial\phi_1}{\partial y}\frac{\partial\phi_2}{\partial y} + \frac{\partial T_1}{\partial x}\left(\frac{\partial\phi_2}{\partial t} + \frac{\partial\phi_1}{\partial t_1} - \kappa\frac{\partial^2\phi_2}{\partial y^2}\right)\\ &+ \frac{\partial T_2}{\partial x}\left(\frac{\partial\phi_1}{\partial t} - \kappa\frac{\partial^2\phi_1}{\partial y^2}\right) - 2\kappa\left(\frac{\partial\phi_1}{\partial y}\frac{\partial^2 T_2}{\partial y\partial x} + \frac{\partial\phi_2}{\partial y}\frac{\partial^2 T_1}{\partial y\partial x}\right)\\ &+ \kappa\left(\frac{\partial\phi_1}{\partial y}\right)^2\frac{\partial^2 T_1}{\partial x^2},\end{aligned}$$

$$\begin{aligned}N_{11} &= 1 - \frac{q^2c_c^2}{2}F''(\hat{T}_b),\\ N_{12} &= -\hat{u}^2,\\ P_{11} &= 2N_{11},\\ P_{12} &= \frac{q^2c_c^2}{2}\left(\frac{1}{\hat{u}}F''(\hat{T}_b)N_{11} + \frac{qc_c}{3}F'''(\hat{T}_b)\right),\\ P_{13} &= \frac{q^2c_c^2}{2\hat{u}}F''(\hat{T}_b)N_{12} + 2\hat{u},\\ P_{14} &= -2\hat{u}^2,\\ N_{21} &= \mathcal{P}N_{11} + q^2c_c\hat{u}f''(\hat{T}_b),\\ N_{22} &= \mathcal{P}N_{12},\\ P_{21} &= \mathcal{P}P_{11} + 2q^2c_c\hat{u}f''(\hat{T}_b),\\ P_{22} &= \mathcal{P}P_{12} - q^2c_cf''(\hat{T}_b)N_{11} - \tfrac{1}{3}q^3c_c^2\hat{u}f'''(\hat{T}_b),\\ P_{23} &= \mathcal{P}P_{13} - q^2c_cf''(\hat{T}_b)N_{12},\\ P_{24} &= \mathcal{P}P_{14},\\ N_{31} &= \tfrac{1}{2}N_{21} + \mathcal{P},\\ N_{32} &= \tfrac{1}{2}N_{22} + \hat{u}^2\mathcal{Z}^*,\\ P_{31} &= \tfrac{1}{2}P_{21} + 2\mathcal{P},\end{aligned}$$

$$P_{32} = \frac{1}{2}P_{22} - \frac{1}{2\hat{u}}N_{21},$$
$$P_{33} = \frac{1}{2}P_{23} - \frac{1}{2\hat{u}}N_{22} - \hat{u}(\mathcal{Z}^* - \mathcal{P}),$$
$$P_{34} = \tfrac{1}{2}P_{24} + 2\hat{u}^2\mathcal{Z}^*$$

Appendix B. Solutions to initial-value problems

The solution T_2, ϕ_2 in (65), (66) to the $O(\epsilon^2)$ problem depends on the functions $g_j(x)$ and constants $C_j,\ j = 0, 2$, which satisfy the initial-value problems (67)–(69). Solutions to the initial-value problems are

$$g_j(x) = \begin{cases} a_{j1}e^{Y_{j+}x} + D_{j1}e^{\hat{u}x/\kappa} + D_{j2}xe^{\hat{u}x/\kappa} + D_{j3}e^{r_+x}, & x < 0 \\ a_{j2}e^{Y_{j-}x} + D_{j4}e^{r_-x}, & x > 0 \end{cases}, \tag{B.1}$$

where

$$Y_{2\pm} = \frac{\hat{u} \pm \sqrt{\hat{u}^2 + 8i\psi\kappa}}{2\kappa}, \qquad Y_{0\pm} = 0,$$

$$D_{21} = \frac{qc_c\mathcal{Z}^*\hat{u}^2(2C_2\kappa + \hat{u})}{2\kappa^2},$$
$$D_{22} = 0,$$
$$D_{23} = -\frac{qc_cr_+(\hat{u}^2\mathcal{Z}^* + i\psi\kappa)}{\kappa},$$
$$D_{24} = -iqc_cr_-\psi,$$
$$D_{02} = \frac{qc_c\mathcal{Z}^*\hat{u}\,(i\psi\hat{u} + r_0\kappa)}{\kappa^2},$$
$$D_{03} = D_{23},$$
$$D_{04} = D_{24},$$

and $r_\pm$ are the expressions in (29) evaluated at $j = 0$. When $j = 2$, applying initial conditions (68) and (69) determines a_{21}, a_{22}, and C_2. When $j = 0$, applying initial conditions (68) and (69) determines a_{01}, a_{02}, and D_{01}.

References

1. D. A. SCHULT and V. A. VOLPERT, Linear stability analysis of thermal free radical polymerization waves, *Int. J. Self-Propag. High-Temp. Synth.* 8:417–440 (1999).

2. A. G. Merzhanov, Theory and practice of SHS: State of the art and newest results, *Int. J. Self-Propag. High-Temp. Synth.* 2:113–158 (1993).
3. K. G. Shkadinsky, B. I. Khaikin, and A. G. Merzhanov, Propagation of a pulsating exothermic reaction front in the condensed phase, *Combust. Expl. Shock Waves* 7:15–22 (1971).
4. A. G. Merzhanov, I. P. Borovinskaya, and A. K. Filonenko, New phenomena in combustion of condensed systems, *Dokl. Akad. Nauk USSR* 208:122–125 (1973) (Engl. Transl. *Sov. Phys. Dokl.* 892–894).
5. Y. B. Zeldovich, O. I. Leypunsky, and V. B. Librovich, *Theory of Non-steady Powder Combustion*, Nauka, Moscow, 1975.
6. B. J. Matkowsky and D. O. Olagunju, Traveling waves along the front of a pulsating flame, *SIAM J. Appl. Math.* 42:486–501 (1982).
7. M. R. Booty, S. B. Margolis, and B. J. Matkowsky, Interaction of pulsating and spinning waves in condensed phase combustion, *SIAM J. Appl. Math.* 46:801–843 (1986).
8. S. B. Margolis, Transition to nonsteady deflagration in gasless combustion, *Prog. Energy Combust. Sci.* 17:135–162 (1991).
9. S. B. Margolis, Chaotic combustion of solids and high density fluids near points of strong resonance, *Proc. R. Soc. A* 433:130–150 (1991).
10. N. M. Chechilo, R. J. Khvilivitskii, and N. S. Enikolopyan, The phenomenon of propagation of the polymerication reaction, *Dokl. Akad. Nauk USSR* 204:1180 (1972).
11. I. R. Epstein and J. A. Pojman, Overview: Nonlinear dynamics related to polymeric systems, *Chaos* 9:255–259 (1999).
12. S. E. Solovyov, V. M. Ilyashenko, and J. A. Pojman, Numerical modeling of self-propagating polymerization fronts: The role of kinetics on front stability, *Chaos* 7: 331–340 (1997).
13. J. A. Pojman, A. M. Khan, and V. M. Ilyashenko, Spin mode instabilities in propagating fronts of polymerization, *Physica D* 84:260–268 (1995).
14. J. Masere, F. Stewart, T. Meehan, and J. A. Pojman, Period-doubling behavior in frontal polymerization of multifunctional acrylates, *Chaos* 9:315–322 (1999).
15. C. A. Spade and V. A. Volpert, Linear stability analysis of non-adiabatic free-radical polymerization waves, *Combust. Theory Modelling* 5:21–39 (2001).
16. L. D. Landau, On the problem of turbulence, *C. R. Acad. Sci., URSS* 44:387–391 (1944).
17. L. D. Landau and E. M. Lifshitz, *Fluid Mechanics*, Pergamon Press, New York, 1959.
18. J. T. Stuart, On the nonlinear mechanisms of wave disturbances in stable and unstable parallel flows—Part I, *J. Fluid Mech*. 9:353–370 (1960).
19. L. K. Gross, Weakly nonlinear dynamics of interface propagation, *Stud. Appl. Math.*, 108:323–350 (2002).
20. L. K. Gross, Weakly nonlinear dynamics of interface propagation, Ph.D. Thesis, Rensselaer Polytechnic Institute, Troy, NY, 1997.
21. M. Garbey, H. G. Kaper, G. K. Leaf, and B. J. Matkowsky, Quasi-periodic waves and the transfer of stability in condensed phase surface combustion, *SIAM J. Appl. Math.* 52:384–395 (1992).
22. J. Kevorkian and J. D. Cole, *Perturbation Methods in Applied Mathematics*, Springer-Verlag, New York, 1996.
23. P. M. Goldfeder, V. A. Volpert, V. M. Ilyashenko, A. M. Khan, J. A. Pojman, and S. E. Solovyov, Mathematical modeling of free-radical polymerization fronts, *J. Phys. Chem.* 101:3474–3482 (1997).

24. B. J. MATKOWSKY and G. I. SIVASHINSKY, Propagation of a pulsating reaction front in solid fuel combustion, *SIAM J. Appl. Math.* 35:230–255 (1978).

25. G. ODIAN, *Principles of Polymerization*, John Wiley and Sons, New York, 1991.

26. C. A. SPADE and V. A. VOLPERT, On the steady state assumption in frontal polymerization, *Chem. Eng. Sci.* 55:641–654 (2000).

THE UNIVERSITY OF AKRON
NORTHWESTERN UNIVERSITY

(Received May 17, 2002)